

Original Article

The Axonal Regeneration Across a Honeycomb Collagen Sponge Applied to the Transected Spinal Cord

Kazuyuki Fukushima¹, Mitsuhiro Enomoto¹, Shoji Tomizawa¹, Makoto Takahashi¹, Yoshiaki Wakabayashi¹, Soichiro Itoh¹, Yoshinori Kuboki^{2,3} and Kenichi Shinomiya¹

1) Department of Orthopaedic and Spinal Surgery, Tokyo Medical and Dental University Graduate School 1-5-45 Yushima Bunkyo-ku Tokyo, 113-8519 Japan

2) Emeritus Professor, Hokkaido University Kita 13 Jo Nishi 7 Chome Kita-ku Sapporo, 060-8586 Japan

3) Koken bioscience institute 2-13-10 Ukima Kita-ku Tokyo, 115-0051 Japan

We developed a honeycomb-shaped lyophilized Type I atelocollagen (Honeycomb Collagen: HC) with different pore sizes, and the effectiveness of the honeycomb shape on nerve regeneration was examined. We analyzed neurite outgrowth of dorsal root ganglion (DRG) explants on HC, both *in vitro* and, with direct implantation of HC into the defects of adult rat spinal cords, *in vivo*. The neurites of DRGs on HC extended linearly through the pores. HC with a 400 μ m-pore size enhanced neurite extension, and YIGSR laminin peptide coating to the HC extended more neurites than fibronectin coating. The HC scaffolds coated with YIGSR were implanted into 2 mm-defects of spinal cords at the level of T8-9. Four weeks after implantation, the implants had degraded and been replaced with self-tissues, repairing the injured site. Neurofilament-positive fibers were observed in the implantation area and passed the borders between the HC and spinal cord stumps. Functionally, a motor-evoked potential was observed in the quadriceps femoris muscle 10 weeks after implantation. The electrophysiological examination showed reconstruction of axon

tracts over the implant. This result indicates that our developed honeycomb shape is advantageous for host spinal cord compared to the random pored sponge shape, and that it promotes axonal regeneration after spinal cord injury.

Key words: spinal cord injury, biomaterial, regeneration, collagen, axonal guidance

Introduction

Spinal cord injury (SCI), which causes para- or tetraplegia, was previously believed to be an incurable trauma. This belief was based on the so-called “central dogma” idea that the injured central nervous system would never recover¹. However, recent studies have shown axonal regeneration and functional recovery after SCI in experimental models. A number of research projects have achieved remarkable breakthroughs, including clinical application of these techniques².

To improve fully functional regeneration after SCI, an appropriate extracellular matrix (ECM) is necessary. Some groups have focused on a scaffold to cover or fill the injured site, and have shown histological and functional improvement after SCI. The use of polyacrylonitril/polyvinylchloride (PAN/PVC) was reported with Schwann cell transplantation³. This study showed successful axonal regeneration after implantation. However, PAN/PVC is not degradable and might

Corresponding Author: Mitsuhiro Enomoto
Department of Orthopaedic and Spinal Surgery, Tokyo Medical and Dental University Graduate School 1-5-45 Yushima Bunkyo-ku Tokyo, 113-8519 Japan
Phone: 81-3-5803-5279 Fax: 81-3-5803-5281
E-mail address: enomoto.orth@tmd.ac.jp
Received October 11; Accepted November 30, 2007

be harmful for long term use. Polylactic acid (PLA), poly-lactic-co-glycolic acid (PLGA), agarose, and collagen filaments are biodegradable materials and have been used in previous studies to fill spinal cord gaps⁴⁻⁷. The handling and preparation of PLA and PLGA are simple, but they persist for a long period of time and may inhibit healing processes⁸. We hypothesized that the ideal artificial ECM for axonal regeneration should perform well in the following three characters: (1) initial strength, (2) axonal guidance ability, and (3) the ability to be replaced by self-tissue at the optimum time.

We have developed an artificial ECM named Honeycomb Collagen (HC)⁹. HC was made from lyophilized Type I atelocollagen and possesses a serial tunnel structure. The applicability of HC for regeneration was demonstrated in an intervertebral disc and cartilage studies^{10,11}. However, nerve regeneration with HC scaffolds remains unclear. An appropriate pore size of HC and coating proteins to HC should be considered as a part of basement membrane composed of nerve structure. We first prepared HC scaffold with different pore sizes and different coating molecules, fibronectin or YIGSR laminin peptide. Neurite extension was evaluated from dorsal root ganglions (DRGs) into each scaffold *in vitro*. We investigated each pore size of

HCs to promote neurite extension *in vitro*, and tested whether implantation of the HC would be appropriate for spinal cord regeneration.

Materials and Methods

Preparation of honeycomb collagen

The generation and characterization of the atelocollagen honeycombs (KOKEN Inc., Tokyo, Japan) has been described previously⁹. Briefly, type I atelocollagen from bovine dermis in solution (1%, pH 3) was poured into a shallow tray and exposed to ammonia gas in order to neutralize it. The resulting white gel was rinsed with distilled water in order to wash out excess ammonia and salt produced during the neutralization reaction. The white gel was freeze dried, and the resulting honeycomb-shaped sponge was sliced into pieces of 2 mm-thickness. The HC was cross-linked for 4 hours in the formalin gas to control the degradation speed in the organism. The pore size of the HCs was controlled with the condition of the freezing speed. The products have a 3-D structure in a uni-directional porous pattern (Fig. 1A). We developed collagen-scaffolds with three different pore sizes with diameters

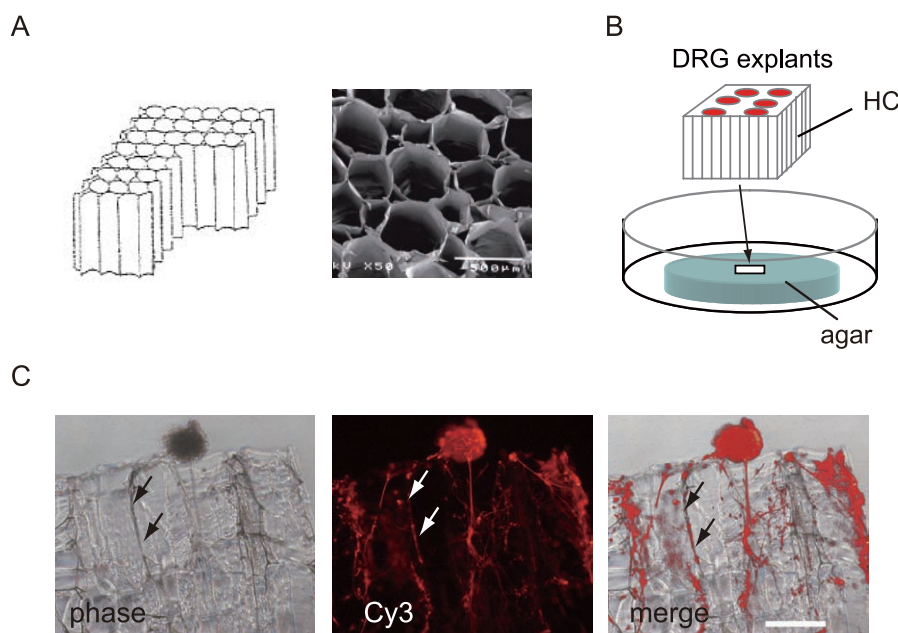


Fig. 1. Appearance of honeycomb collagen sponge (HC) and *in vitro* evaluation of DRGs on HC (A) HC consists of serial tunnel structures like a honeycomb. (B) HC with DRG explants was held by an agarose gel. Red circles show DRG explants. (C) 300 μ m-sections were obtained with DRGs and HC. NF-positive fibers (red) from a DRG explant entered straightly into the pores of the HC (arrows). Scale bar, 300 μ m.

of 130 μm (HC130), 200 μm (HC200), and 400 μm (HC400). We cut the HC into pieces of 2 mm length and width under the microscope. Randomly pored collagen (RPC) was prepared without a uni-directional porous pattern as a control.

Coating HC with ECM proteins

Pieces of HC and RPC were soaked in one of two ECM proteins, either 100 $\mu\text{g}/\text{ml}$ of a YIGSR laminin peptide, the minimum recognition sequence for laminin-1's 67-kDa receptor (BACHEM, Bubendorf, Switzerland),¹² or fibronectin (Sigma, St Louis, USA). They were defoamed at 100 mmHg using a vacuum pump for 10 min, centrifuged at 7000 rpm, and defoamed again for 10 min. The coated HCs and RPCs were dried overnight at 4 °C before experiments. All implants were coated with YIGSR peptide. The other set of HC400 coated with fibronectin was prepared for comparison with YIGSR peptide.

Cultivation of DRG on HC

The animal care committee of Tokyo Medical and Dental University approved all animal experiments. E16 pregnant female SD rats were sacrificed by decapitation under ether anesthesia, and embryos were removed immediately. Spinal cords with dorsal root ganglions (DRGs) were removed from vertebral bodies, and DRGs were carefully removed from spinal cords as close to the ganglia as possible. To stabilize collagen sponges on culture dishes, we established a cubic framework made of 2% agar in phosphate buffered saline (PBS) with a center hole of 3 mm-diameter, and attached it to the bottom of the culture dish before preparing the DRGs (Fig. 1B). Collagen sponges presoaked in 0.1 M PBS were placed inside molded agar and filled with DRG medium, which contained DMEM/F12 (Gibco, San Diego, USA), Hepes (Gibco), insulin (5 mg/l, Sigma), 5 mM phosphocreatinin (Sigma), sodium pyruvate (400 mg/l, Sigma), sodium selenite (5 $\mu\text{g}/\text{l}$, Sigma), apo-transferin (100 mg/l, Sigma), 1% penicillin-streptomycin, 100 nM progesterone and 15 ng/ml nerve growth factor (NGF) (CHEMICON, Temecula, USA). The ideal pore size was examined preceding implantation into the spinal cord. We prepared HCs with different pore sizes of a 130 μm diameter (HC130), 200 μm diameter (HC200), and 400 μm diameter (HC400), and cultured DRGs on them for 6 days (Fig. 2). The experiments were repeated three times. (total DRG numbers on RPC = 12, HC130 = 24, HC200 = 42, HC400 = 48, HC400 coated with YIGSR = 48, and HC400 coated with

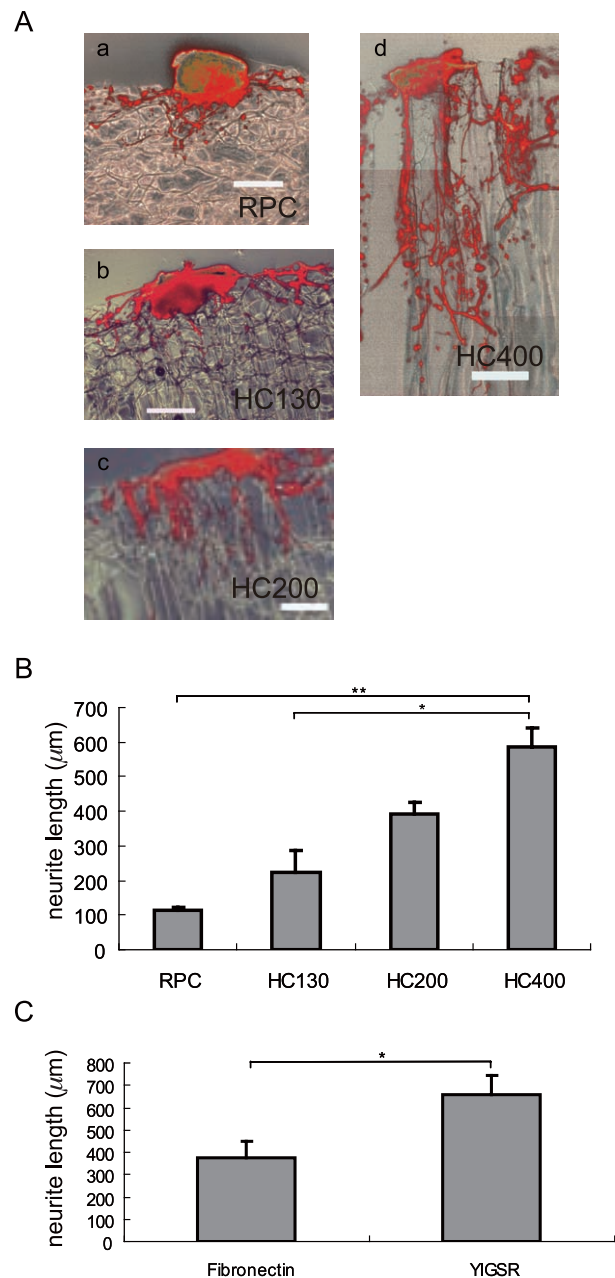


Fig. 2. (A) Evaluation of neurite length from DRG explants into HC pores NF-positive fibers from DRG explants on honeycomb collagen sponges (HC) with different pore sizes (a, b, c and d). Scale bar, 300 μm . (B) Quantification of neurite length entering the HC coated with YIGSR (total DRG numbers on RPC = 12, HC130 = 24, HC200 = 42, HC400 = 48). The length of neurites sprouting into HC400 was significantly longer than that sprouting into HC130 and RPC. Significant difference; * $p < 0.05$, ** $p < 0.01$, Bonferroni's post hoc test (C) Quantification of neurite length entering HC400 coated with fibronectin and YIGSR (total DRG numbers on HC400 coated with fibronectin = 24, HC400 coated with YIGSR = 48). The length of neurites sprouting into HC400 coated with YIGSR was significantly longer than that sprouting into HC400 coated with fibronectin. Significant difference; * $p < 0.05$, Student's t-test.

fibronectin = 24). The medium was changed every 3 days.

Immunocytochemistry of the DRG neurites

The HCs and RPCs with DRGs were fixed with 2% paraformaldehyde (PFA) in PBS for 30 min. After treatment with 0.5% Triton X in PBS for 5 min, the DRGs with scaffolds were blocked with 5% NGS and incubated with an anti-neurofilament (NF) 200 antibody (1:40, Sigma). The primary antibody was visualized with goat anti-mouse IgG conjugated to Cy3 (1:200, Jackson ImmunoResearch, West Grove, USA). Immunostained collagen sponges with DRGs were embedded in 1.2% agar in PBS, and a 300 μ m section was taken with a microtome. The sections were placed on a coverslip and observed with a fluorescent microscope (OLYMPUS IX70, Tokyo, Japan). These images were processed with Adobe Photoshop (Adobe systems Incorporated, San Jose, USA). The lengths of all neurites along the holes of the collagen sponges were measured with a Scion image (Scion Corporation, Frederick, USA). The total length of the neurites from each DRG explant was measured in all sections containing neurites and then averaged.

Implantation of the collagen sponges

Under intraperitoneal chloral hydrate anesthesia (350 mg/kg, Wako Chemical Industries, Osaka, Japan), female SD rats at the age of 9 weeks were placed on a heat pad. A laminectomy was performed at the T8-9 vertebral level. The exposed T8-9 spinal cord was completely transected along 2 mm with an ophthalmic blade. After hemostasis was achieved, a 2 mm-long scaffold of HC400 ($n = 6$) or RPCs ($n = 5$) was implanted between the rostral and caudal spinal cord stumps. The stumps and implant were covered with fibrin glue (Tisseel®, Baxter, Deerfield, USA). The muscle and skin were closed with 5-0 nylon. A bladder-skin fistula was applied to prevent renal failure after surgery. An adhesive bandage was placed on the lower half of the belly of the rat, and rat repellent paint (Naramysin; Nakagawasanngyo, Osaka, Japan) was painted onto the bandage to prevent autophagia. To prevent urinary tract infection and renal failure, 0.6 ml of vytril and 10 ml saline were administered daily during the first 7 days after surgery.

Immunohistochemistry of the implanted spinal cords

Four weeks after implantation, animals were anesthetized with terminal chloral hydrate anesthesia (600

mg/kg body weight) and perfused transcardially with 100 ml of 0.1 M PBS followed by 500 ml of 2% PFA in 0.1 M PBS (pH 7.4). A 14 mm long spinal cord section, containing the implant, was dissected under a microscope. The spinal cords were embedded in 1.2% agarose in 0.1 M PBS after dehydration with sucrose solutions. Sagittal sections (30 μ m) through the scaffolds were cut on a cryostat, mounted onto glass slides, and stored at -20 °C until further processing. Cryostat sections were permeabilized with 0.5% Triton X in PBS for 3 min, blocked with 5% NGS for 30 min, and incubated with anti-NF 200 antibody (1:40, Sigma) for 3 hours. The secondary antibody incubation was performed with goat anti-mouse IgG conjugated to Cy3 (1:200, Jackson ImmunoResearch, West Grove, USA) for 2 hours. Images were obtained on an OLYMPUS IX70.

Quantitative evaluation of the neurites in the implanted HC or RPC

A total of approximately 45 slices per spinal cord were examined. We divided these sections into three groups. Each group included 15 sections from the left to right lateral sides. We selected three serial sections from the middle section of each group (e.g., section # 7, 8, 9, 22, 23, 24, 36, 37, 38). Images were obtained, and the number of NF-positive fibers were counted and analyzed in the three areas over which the implant was equally divided: the rostral, middle, and caudal areas.

Electrophysiological evaluation

Ten weeks after implantation, the motor-evoked potential (MEP) was measured by Neuropack 8 (Nihon Kohden, Tokyo, Japan). The stimulus electrodes were placed in the skin of the head just above the sensory-motor cortex under intraperitoneal chloral hydrate anesthesia. The needle electrodes were stuck into the tendon origin, the quadriceps femoris muscle, and the gastrocnemius muscle, and also into the forearm muscle as a positive control. The stimulus intensity was 5 mA, and train stimulation was loaded 3 times. After the measurement of MEP, the spinal cord was exposed at Th12 and retransected to prove the connection of descending pathways beyond the implant.

The MEP was measured similarly after retranssection.

The statistical analysis

Multiple comparisons of the average number of neurite length among HCs with different pore sizes were carried out using the Bonferroni's post hoc test (the Statcel add-in program for Microsoft Excel). An

unpaired student's t-test was used to determine statistical differences between the average number of neurite lengths in HC400 coated with fibronectin and YIGSR *in vitro*. The Mann-Whitney U test was used to determine statistical differences between the average number of NF-positive fibers in HC400 and RPC coated with YIGSR *in vivo*. Data represent means \pm S.D.

Results

The comparison of the neurite length in the different pore sizes of honeycomb collagen sponges

Honeycomb collagen sponges (HCs) had a uni-directional porous pattern (Fig. 1A). DRG explants extended their neurites toward the pores of the HCs after 6 days *in vitro*. In longitudinal 300 μ m sections, NF-positive neurites were observed along the walls of the pores inside the HCs (Fig. 1C). We analyzed neurite length extended from DRGs into HCs with different pore sizes of a 130 μ m diameter (HC130), 200 μ m diameter (HC200), and 400 μ m diameter (HC400) (Fig. 2A). The length was $224.9 \pm 60.8 \mu$ m in HC130, $392.3 \pm 34.6 \mu$ m in HC200, $586.0 \pm 56.1 \mu$ m in HC400 and $112.6 \pm 9.9 \mu$ m in RPC (Fig. 2B). The neurite length sprouting into HC400 was significantly longer than that in HC130 and RPC. There was a tendency for the length in HC400 to be longer than in HC200, and thus we chose to use HC400 in the next experiment.

The comparison between the YIGSR and fibronectin coating to HCs *in vitro*

We tested two ECM molecules to coat the HCs for providing an environment for regenerating axons. The length of neurites sprouting into HC400 coated with fibronectin was $377.3 \pm 69.7 \mu$ m, while the length with YIGSR was $661.1 \pm 81.8 \mu$ m. Statistical analysis revealed that the length of the neurites sprouting into HC400 coated with YIGSR was significantly longer than that observed with fibronectin (Fig. 2C).

Implantation of HC coated with YIGSR in a rat SCI model

HCs with a 400 μ m pore size were treated with YIGSR and implanted into the 2 mm-gap of thoracic spinal cords. We observed the degradation and replacement of the HCs with H.E. staining. The collagens still remained after 2 weeks, but disappeared almost completely after 4 weeks (Fig. 3A). Tissue with a funicular pattern replaced the HCs within the

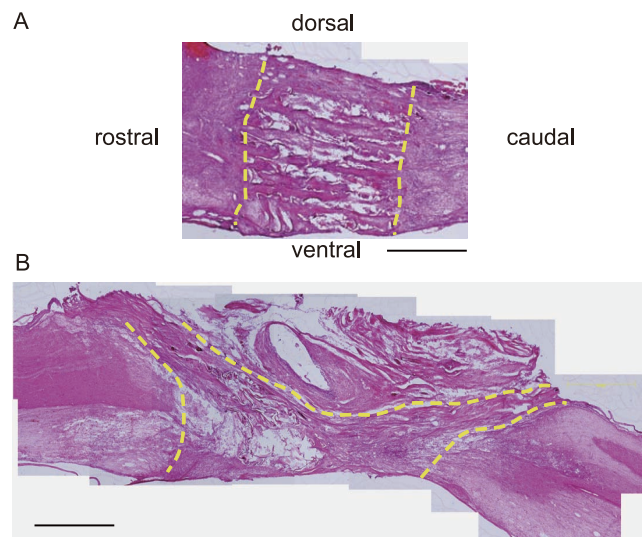


Fig. 3. H.E. staining of spinal cord-implanted honeycomb collagen (A) The implanted site of an HC400 coated with YIGSR was observed 2 weeks after implantation, and (B) 4 weeks after implantation. The yellow dotted lines show the border between the implant and the spinal cord. Scale bar, 1 mm.

implanted areas and bridged the gap between proximal and distal spinal cord stumps (Fig. 3B).

Immunohistochemical analysis with neurofilament positive fibers in the spinal cord

In RPCs, NF-positive fibers entered into the implanted site, but very few fibers crossed the rostral border (Fig. 4A). In contrast, NF-positive fibers were observed beyond the borders between the HCs coated with YIGSR peptide and the host spinal cords 4 weeks after implantation (Fig. 4B). At higher magnification, many NF-positive fibers were observed and arranged parallel to the longitudinal direction in the middle of the implants (Fig. 4D), while several fibers were seen to cross the border between the implanted area and the stumps (Fig. 4C and E). The numbers of NF-positive fibers in three equally divided areas were counted. In the HCs, the number of fibers was 41.5 ± 13.5 in the rostral area, 17.7 ± 4.3 in the middle area, and 28.2 ± 9.0 in the caudal area. In the RPCs, the number of fibers was 10.8 ± 5.8 in the rostral area, 1.0 ± 0.8 at the middle area, and 1.4 ± 1.0 in the caudal area (Fig. 4F). More NF-positive fibers were present in the middle and caudal areas in the case of HCs.

Muscle-evoked potential study 10 weeks after the SCI treated with the HC implant

We examined the rats ($n = 3$) 10 weeks after HC

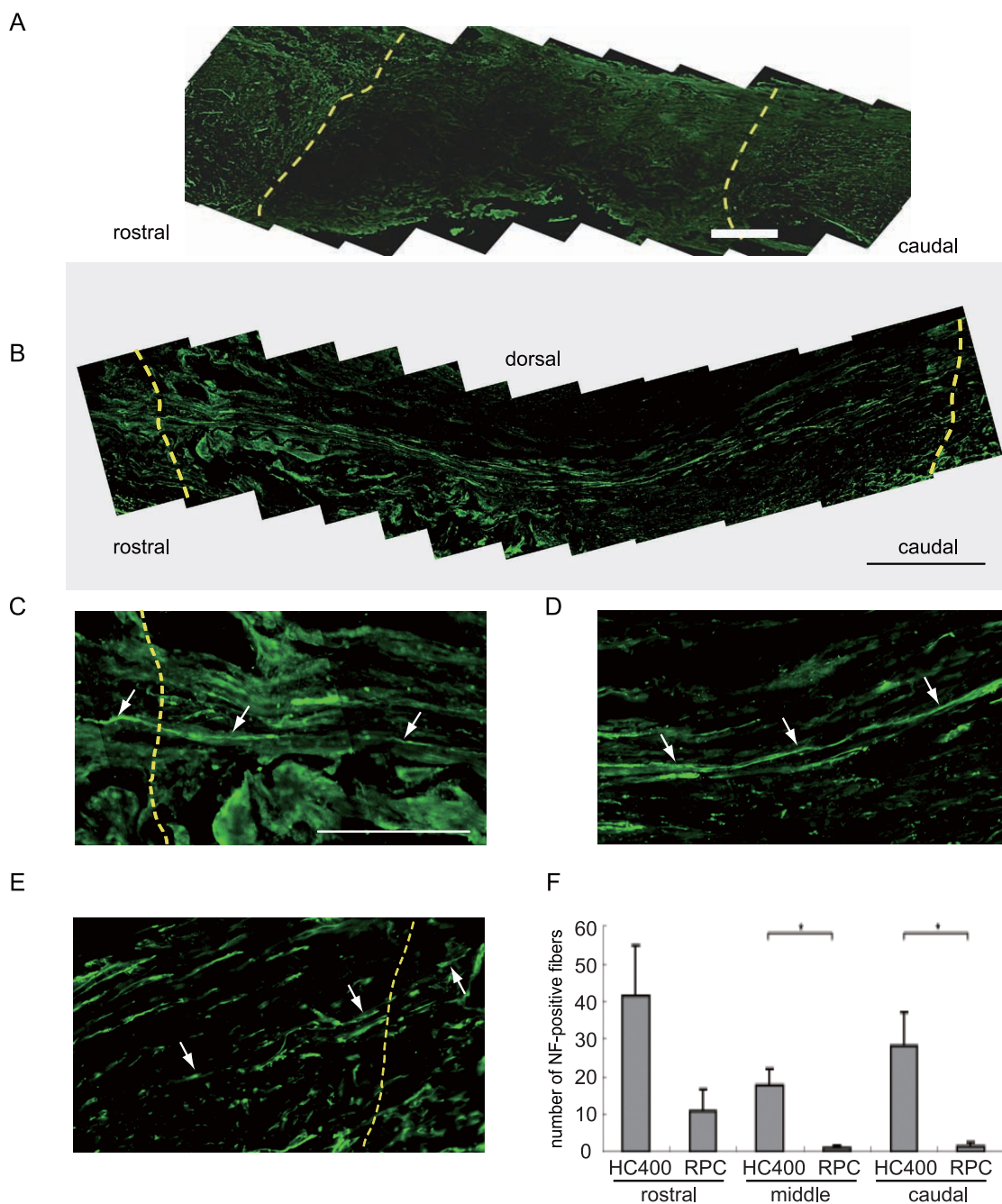


Fig. 4. Implanted spinal cords stained with NF 4 weeks after implantation. The yellow dotted lines show the border between the implant and the spinal cord (A) Few NF-positive fibers were observed within the RPC implanted site. Scale bar, 250 μm . (B) Many NF-positive fibers were shown to be linear, and bridged the length of the spinal cord-implanted HC 400. Scale bar, 250 μm . (C) In a higher magnification view of the rostral border between the HC and the spinal cord, NF-positive fibers (arrows) enter the implanted area across the rostral border between the spinal cord and the HC. (D) In the middle portion, the NF-positive fibers (arrows) were arranged in parallel with the sagittal direction. (E) Some NF-positive fibers (arrows) cross the caudal border between the HC and the spinal cord. (C, D and E, scale bar, 100 μm). (F) Quantification of the NF-positive fibers in the rostral, middle and caudal areas of implanted site. More NF-positive fibers were seen with HC 400 coated with YIGSR ($n = 6$) than with RPC ($n = 5$). Significant difference; * $p < 0.05$, Mann-Whitney U test.

implantation. After transcranial electrostimulation, muscle-evoked potentials (MEPs) were recorded from both quadriceps femoris muscles, and also from the forearm muscle as a control. MEPs were observed in the right quadriceps femoris muscle with HC implantation (Fig. 5A). In the next step, the spinal cord was re-transected at the distal stump. Both MEPs and contraction of the quadriceps femoris muscle disappeared after the transection (Fig. 5B). These results show that a reconnection of some descending pathways across the HC-implanted area had occurred.

Discussion

A number of artificial ECMs with several 3D configurations have been previously studied in the spinal cord injury model³⁻⁷. Although their axon-guidance abilities have been well evaluated, few studies have verified that guidance ability was derived from a 3D structure by comparison with a negative control framework. In recent years, "the geometry of the artificial ECM" has been advocated as a new theory surrounding artificial ECM. In studies of bone and blood vessel regeneration with the use of artificial ECM, Kuboki, *et al.* revealed differences in regenerated tissue depending upon the 3D configuration of the artificial ECM used¹³. In that study, a serial tunnel structure with 300-400 μm pores was the most advantageous for the regeneration of blood vessel and bone. Therefore, we

newly developed honeycomb collagen scaffold with various pore sizes, and hypothesized that the serial tunnel structure could guide regenerated axons in the injured spinal cord in a specific direction.

Our results from DRG cultivation on a HC have revealed a serial tunnel structure with 400 μm pores to be the most advantageous for guiding sprouting neurites. The length of neurites entering artificial ECM pores was strongly dependent upon differences in the 3D configuration of the ECM. We tested two ECM molecules to coat the HCs preceding implantation into the spinal cord. The length of the DRG neurites that entered the YIGSR-coated HC was significantly longer than the fibronectin-coated HC. Laminin and fibronectin are common extra-cellular matrices, but they are difficult to synthesize because of their large molecular weights. The YIGSR peptide is easily synthesized, and has neural outgrowth-promoting activity *in vivo*¹⁴. It has been suggested that the YIGSR peptide acts on the growth cone to promote their attachment and migration in our studies.

In this study, we implanted RPC into the defect of spinal cords as the negative control. First, we set the negative control as only spinal cord defects without an implant. However, all rats had died in the early phase after surgery, and the stumps of the spinal cord had highly atrophied. The defect without implant might have caused continuous bleeding from spinal cord stumps. We tried to implant the material which had the different configuration from the honeycomb shape.

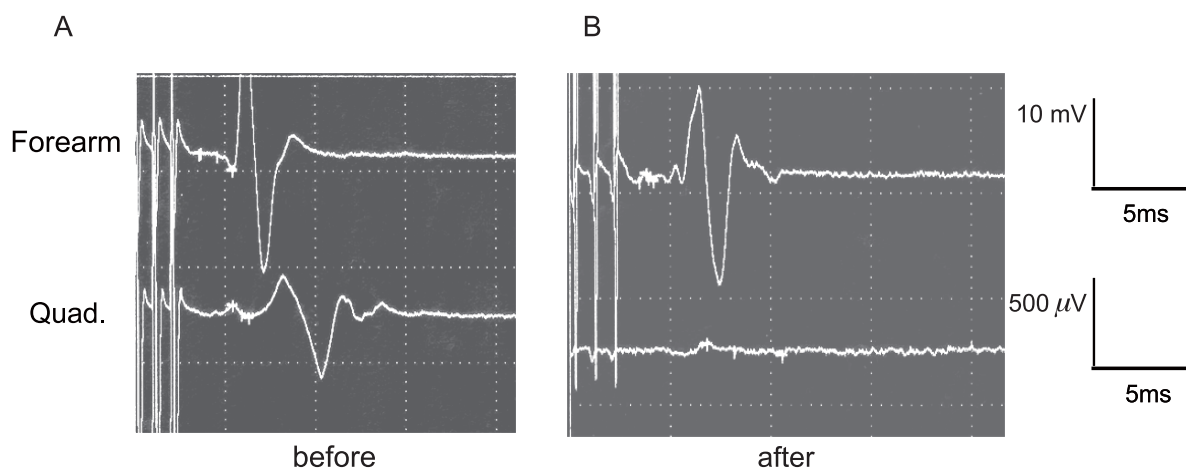


Fig. 5. The motor evoked potential (MEP) of the quadriceps femoris and the forearm muscle at 10 weeks after implantation. (A) The MEPs in forearm (upper) and quadriceps femoris muscles (lower) were observed by trans-cranial electrostimulation in the rat implanted HC400 coated with YIGSR. (B) The positive wave of the MEP was diminished in the quadriceps femoris muscle after retranssection of the caudal spinal cord.

The single and huge tube structure and/or the random shape sponge were conceivable as the negative framework. The fragility of the single tube was reported in the polylactic acid scaffold¹⁵. Therefore, the random shape sponge is appropriate scaffold as a negative control.

The spinal cord implanted HC has shown that a greater number of NF-positive fibers entered the HC with 400 μ m pores coated with YIGSR peptide from the stumps compared to RPC, which lacks honeycomb-shaped pores and prolonged degradation. In other words, the degree of the axonal regeneration after severe injury of the spinal cord depended upon the 3D configuration of the implant. The honeycomb structure could lead to a method of regeneration distinct from conventional ones, including cell transplantation or drug administration.

To evaluate regenerated neurites or axons in implanted HC, we used anti-neurofilament 200 antibody. The GAP43 or MAP2a/b was reported as the specific marker of axons or dendrites respectively. In fact, anti-neurofilament 200 antibody could not distinguish the axons from dendrites, and the origin of the fibers into the implant was unknown in this study. Fenrich *et al.* reported that proximally axotomized spinal interneurons have the potential to form new connections via de novo axons that emerge from distal dendrites in the adult cat spinal cord¹⁷. We considered that the axons emerged from the distal dendrite of the interneuron could enter the HC implanted area in this study.

We tested the motor-evoked potential in the hind limb with trans-cranial electro-stimulation. The train stimulation was used to get over the synapse in the implanted HC. MEPs were confirmed to be present in the hind limb, and disappeared after re-transection of the caudal spinal cord. Wakabayashi *et al.* showed evidence of functional connections according to the disappearance of MEPs by retransection of spinal cord¹⁶. These findings indicated that NF-positive fibers in the transplanted biomaterial were functioning, and that the descending conduction was relayed (or bridged) via the HC.

In summary, the shape of the honeycomb with 400 μ m pores and combination of YIGSR coating peptide were more appropriate for neurite extension *in vitro*. The implantation of the HC into a spinal cord gap induced the regeneration of axons and functional connections. Honeycomb collagen sponge is therefore a promising scaffold for clinical use to fill gaps and cavities of injured spinal cords.

Acknowledgements

This research was partly supported by a Grant-in-Aid for Scientific Research from the Japanese Ministry of Education, Science, Sports, and Culture (No. 16659404). And also this work has been supported by Koken Bioscience Institute in donating several kinds of the artificial ECM. The authors are grateful to Toshio Terashima and Kazuo Watabe for help with histology.

References

1. Cajal SR. Degeneration and Regeneration of the Nervous System. New York: Hafner 1928
2. Thuret S, Moon LD, Gage FH. Therapeutic interventions after spinal cord injury. *Nat Rev Neurosci*. 2006;7:628-643
3. Xu XM, Guenard V, Kleitman N, *et al.* Axonal regeneration into Schwann cell-seeded guidance channels grafted into transected adult rat spinal cord. *J Comp Neurol*. 1995;351:145-160
4. Hurtado A, Moon LD, Maquet V, *et al.* Poly (D,L-lactic acid) macroporous guidance scaffolds seeded with Schwann cells genetically modified to secrete a bi-functional neurotrophin implanted in the completely transected adult rat thoracic spinal cord. *Biomaterials*. 2006;27:430-442
5. Teng YD, Lavik EB, Qu X, *et al.* Functional recovery following traumatic spinal cord injury mediated by a unique polymer scaffold seeded with neural stem cell. *Proc Natl Acad Sci*. 2002;99(5):3024-3029
6. Stokols S, Tuszynski MH. Freeze-dried agarose scaffolds with uniaxial channels stimulate and guide linear axonal growth following spinal cord injury. *Biomaterials*. 2006;27(3):443-51
7. Yoshii S, Oka M, Shima M, *et al.* Bridging a spinal cord defect using collagen filament. *Spine*. 2003;28(20):2346-2351
8. Sung HJ, Meredith C, Johnson C, *et al.* The effect of scaffold degradation rate on three-dimensional cell growth and angiogenesis. *Biomaterials*. 2004;25:5735-5742
9. Itoh H, Aso Y, Furuse M, *et al.* A honeycomb collagen carrier for cell culture as a tissue engineering scaffold. *Artif Organs*. 2001;25(3):213-217
10. Sato M, Asazuma T, Ishihara M, *et al.* Tissue engineering of the intervertebral disc with cultured annulus fibrosus cells using atelocollagen honeycomb-shaped scaffold with a membrane seal (ACHMS scaffold). *Med Biol Eng Comput*. 2003;41(3):365-71
11. Masuoka K, Asazuma T, Ishihara M, *et al.* Tissue engineering of articular cartilage using an allograft of cultured chondrocytes in a membrane-sealed atelocollagen honeycomb-shaped scaffold (ACHMS scaffold). *J Biomed Mater Res B Appl Biomater*. 2005;75(1):177-84
12. Graf J, Iwamoto Y, Sasaki M, *et al.* Identification of an amino acid sequence in laminin mediating cell attachment, chemotaxis, and receptor binding. *Cell* 1987;48(6):989-996
13. Kuboki Y, Jin Q, Takita H. Geometry of carriers controlling phenotypic expression in BMP-Induced osteogenesis and chondrogenesis. *J Bone Joint Surg. Am*. 2001;83:105-115
14. Itoh S, Takakuda K, Samejima H, *et al.* Synthetic collagen fibers coated with a synthetic peptide containing the YIGSR sequence of laminin to promote peripheral nerve regeneration *in vivo*. *J Mater Sci Mater Med*. 1999;10:129-134

15. Oudega M, Gautier SE, Chapon P, Axonal regeneration into Schwann cell grafts within resorbable poly (alpha-hydroxyacid) guidance channels in the adult rat spinal cord. *Biomaterial* 2001;22:1125-36
16. Wakabayashi Y, Komori H, Kawa-Uchi T, *et al.* Functional recovery and regeneration of descending tracts in rats after spinal cord transection in infancy. *Spine*. 2001;26(11):1215-22.
17. Fenrich KK, Skelton N, MacDermid VE, *et al.* Axonal regeneration and development of de novo axons from distal dendrites of adult feline commissural interneurons after a proximal axotomy. *J Comp Neurol*. 2007;502:1079-97